

Unusual electron temperature profile due to grain electrostatics in planetary nebula cored dusty plasma

Hemanga Jyoti Sarmah  †

Department of Physics, Morigaon College, Morigaon, Assam 782105, India

(Received 8 July 2024; revised 11 December 2024; accepted 12 December 2024)

The Cloudy photoionization codes have been employed to study a spherically distributed cloud, around an arbitrary planetary nebula, with core temperature 10^5 K. The ionization factor $\chi(H)$ is close to unity, in the inner face of the dusty plasma (DP) cloud, which follows a monotonic declining trend, afterwards. For hydrogen density $n_H = 10 \text{ cm}^{-3}$, an exponentially falling trend of temperature could be noticed. A grain charging\discharging process is also witnessed, which is very common in a DP environment. For $n_H = 10 \text{ cm}^{-3}$, photoionization of grains is more common due to higher photon density; compared with $n_H > 10 \text{ cm}^{-3}$, where the grain–electron acquiring probability is maximum, because of significant electron density. Owing to the electrostatic interactions between the charged grain and the electrons, an unusual trend in temperature has been observed.

Keywords: dusty plasma, photoionization, planetary nebula, electron temperature

1. Introduction

According to the reports received from the Hubble Space Telescope, a large-scale structure (\sim few parsec (pc)) of dusty plasma (DP), consisting of ions, electrons, gases, dust grains, etc. has been witnessed (Mendis & Rosenberg 1994; Wood & Linsky 1997). Being, a partially or completely ionized system, the properties of the DP is strongly governed by an electric and/or magnetic field, a local field due to charging of the grains or dust particles; in addition to the gravitational field, turbulence, photon flux, etc. (Uzdensky & Rightley 2014). Note that the number density in the DP may vary from $0.01\text{--}10^6 \text{ cm}^{-3}$ (Saintonge & Catarella 2022). Charging of dust grains via photoionization occurs when incident photo-energy exceeds the work function of the grain surface (Fortov *et al.* 2003). In addition to this, the charging of dust grains is also recorded, by accumulation of electrons and/or ions in a DP system (Goree 1992; Abid, Ali & Muhammad 2013). To probe the properties of DP in a stellar environment, researchers mostly rely on the spectroscopic investigations (Dalgarno & Layzer 1987). Apart from the chemical information, physical properties can also be probed from the atomic lines, emission/absorption lines from stellar DP. In the interstellar medium, carbonate, silicate,

† Email address for correspondence: hsarmah94@gmail.com

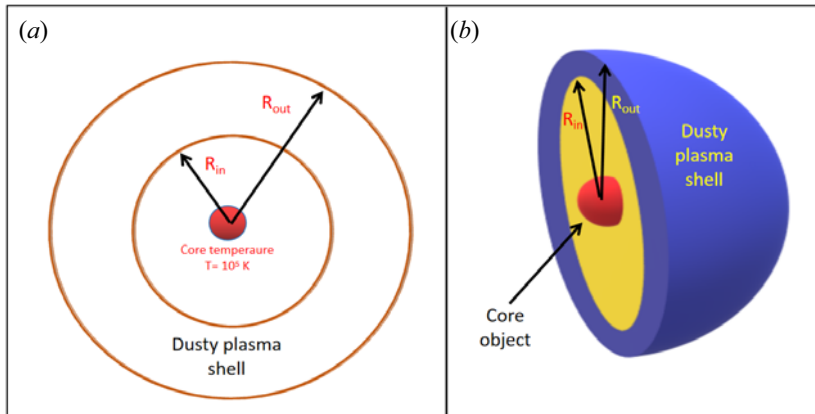


FIGURE 1. A schematic view of the model considered is depicted: (a) 2-D view; (b) 3-D view.

polyaromatic hydrocarbon (PAH), etc. are usually witnessed from the spectroscopic studies (Tielens & Allamandola 1987). Note that most of the studies have confirmed the carbon richness and the presence of PAH around the periphery of a planetary nebula (PN) system (Meixner *et al.* 1993; Guzman-Ramirez *et al.* 2011; Cox *et al.* 2015). Employing the photoionization codes, the temperature profile of dusty PN has been studied, in the existing literature (Stasińska & Szczerba 2001). However, the unusual temperature gradient has not been addressed properly. Prior to Stasińska & Szczerba (2001), the origin of temperature fluctuations was discussed by Liu *et al.*, in a PN environment (Liu & Danziger 1993).

In this work, we have studied the photoionization effects of the PAH dominated DP with varying hydrogen density, in the periphery of PN and probed the origin of the unusual temperature gradient.

2. Theoretical model and tool

A spherically symmetric distribution of cloud containing gas and dust/grains is considered around the PN, assumed to be placed at the core. A schematic diagram in a two-dimensional (2-D) and three-dimensional (3-D) view of the model is depicted in figure 1(a,b). The inner and outer surface radius of the DP shell is taken 1 pc and 3 pc, respectively. Considering PAH domination in the DP, we employed the *pah1_ab08_10.opc* file as input (supplementary material is available at <https://doi.org/10.1017/S0022377824001697>). Estimating an ideal black-body, the temperature and luminosity of the core object are chosen as $T = 10^5$ K and 1.25×10^{38} erg sec⁻¹, respectively; which is consistent with the earlier works (Liu & Danziger 1993). In this work, the hydrogen density of the system is varied from 10 to 10^4 cm⁻³. To study the photoionization of DP and its underlying physics, we have employed the open-source codes from Cloudy (Ferland *et al.* 1998, 2017). The incident spectrum as recorded in the inner face of the DP shell is presented in figure S1 (supplementary material).

3. Result and discussions

3.1. Photoionization in DP

Ferland's Cloudy codes are one of the most promising tools to study the photoionization in a stellar environment (Ferland *et al.* 1998; Salz *et al.* 2015). To illustrate the photon-induced ionization, we define ionization factor $\chi(H) = N(HII)/n_H$; where $N(HII)$

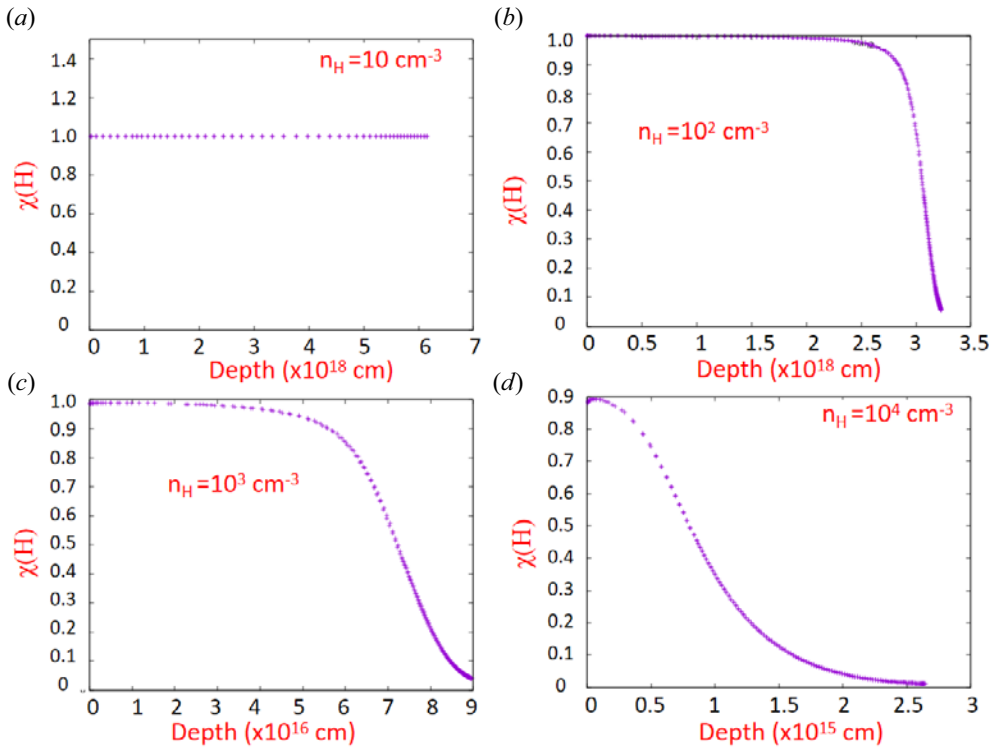


FIGURE 2. The ionization profile of hydrogen for different hydrogen density conditions.

and n_H are the density of H^+ ions and total hydrogen, respectively. The plot for $\chi(H)$ as a function of depth is depicted in figure 2(a–d). For higher hydrogen density values, a declining trend of $\chi(H)$ is recorded, which may be attributed due to reducing intensity and red-shifting of the photons as a consequence of multiple collisions with the atoms, molecules or dust. A similar trend is also recorded for electron density (n_e), as it mostly depends on the $\chi(H)$ (figure 3a–d). Note that for photoionization, the energy of the incident photon ($h\nu$) must be greater than the threshold energy (ϕ_{th}) of the system. The kinetic energy of the photoionized electrons can be expressed as (Güémez & Fiolhais 2018)

$$T_p = h\nu - \phi_{th}, \tag{3.1}$$

where, T_p is the kinetic energy of the photoionized electrons.

3.2. Dusty plasma thermal properties effected by the electrostatics of the dust/grains

The Cloudy codes were also used to probe the thermal properties of the DP. The temperature profile in DP is presented in figure 4(a–d) for different hydrogen density $10\text{--}10^4 \text{ cm}^{-3}$. The DP with lower hydrogen density ($n_H = 10 \text{ cm}^{-3}$) shows a monotonic decreasing trend of temperature with depth of DP (figure 4a). Apart from the inverse square fall of radiation intensity, it also red shifted due to multiple collisions between photon and DP constituent particles; which is speculated for a monotonic lowering trend of temperature in the case $n_H = 10 \text{ cm}^{-3}$. Note that similar trends have been witnessed in the existing literature (Liu & Danziger 1993). As can be seen from figure 4(b–d), the temperature profile exhibits three different regions, for DP with higher $n_H (> 10 \text{ cm}^{-3})$. In the first region, the temperature drops monotonically, a bump can be witnessed in the

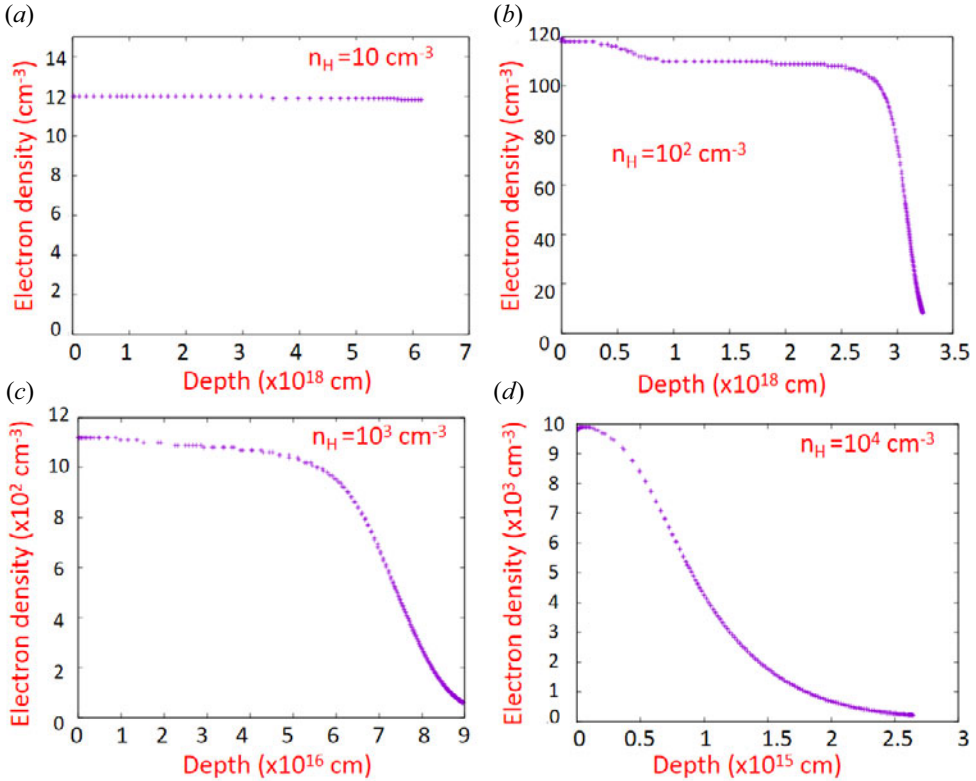


FIGURE 3. Variation of electron density with depth of the DP system. Note that a declining trend of electron density is witnessed with depth for $n_H = 10^2 - 10^4 \text{ cm}^{-3}$; the electron density remains almost unchanged for $n_H = 10 \text{ cm}^{-3}$.

second region, a sharp drop in temperature can be recorded in the third region. It is well established that the electron temperature is co-related to its velocity as $v_e = \sqrt{k_B T_e / m_e}$. Note that in a PN DP environment, the velocity of the electron depends on three factors: first, the gradient dependent flow (diffusion velocity $\propto \Delta n$), i.e. the diffusion; second, electrostatic drift due to the presence of the ionized PAH grains which is present in the DP; and finally, due to the photo-energy absorption process, as mentioned in Section (3.1). Considering all these factors, the net kinetic energy of electrons can be expressed as

$$T_{\text{net}} = T_p + T_d + \beta d_g \phi_{\text{el}} - \Gamma, \quad (3.2)$$

$$\Rightarrow T_{\text{net}} = h\nu - \phi_{\text{th}} + \alpha \Delta n_e^2 + \beta d_g \phi_{\text{el}} - \gamma n \Delta r. \quad (3.3)$$

Here, d_g is the dust-to-gas ratio, the kinetic energy due to diffusion and electrostatic dust potential are termed as $T_d = \alpha \Delta n_e^2$ and ϕ_{el} respectively. Here α , β and γ are constants. The energy loss due to inelastic collisions or scattering is termed as $\Gamma = \gamma n \Delta r$, which is speculated to be increased with depth (Δr) of the DP medium, along with the number density of the system owing to multiple collisions. Considering, $\alpha = 0.00002$, $\beta = 10^5$ and $\gamma = 0.36 \times 10^{-18}$, the plots for T_{net} in accordance to (3.3) have been presented in figure S2(a,b) (supplementary material), which is similar to the temperature profile (figure 4a,d) for $n_H = 10 \text{ cm}^{-3}$ and 10^4 cm^{-3} , respectively. The same is also true for other hydrogen

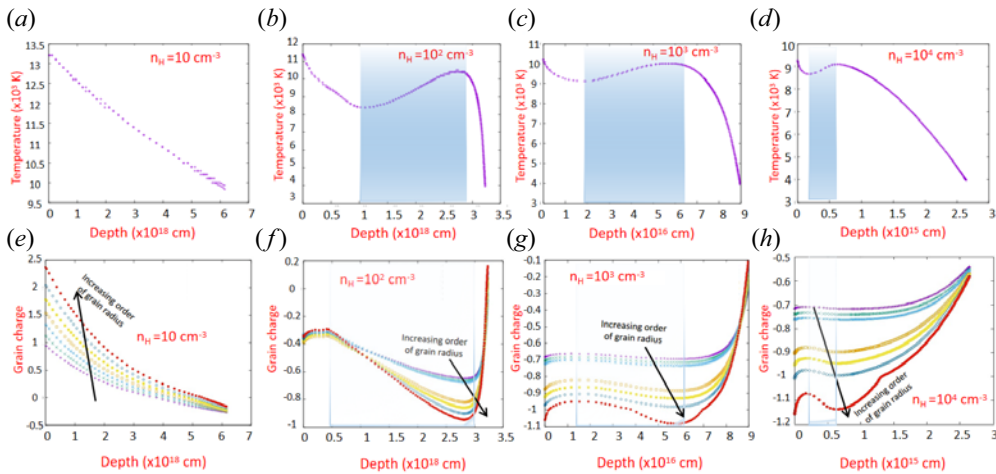
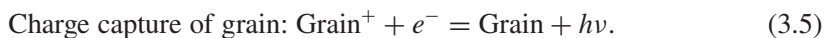
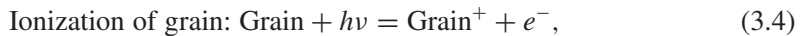


FIGURE 4. (a–d) Electron temperature variation in DP for different hydrogen density condition. (e–h) The variation of average grain charge (in units of electronic charge per grain) is depicted for different hydrogen densities. In the figure, different colours correspond to grains of different radius (average); the increasing order of grain radius is shown with an arrowhead. Note that the average grain charge is the mean value of different charge states of a particular grain of shape and size in each zone.

density conditions (not shown). Further details can be found in the supplementary material.

The grain charging/discharging processes are quite common in a DP environment. The basics process of ionization/charge capture processes are depicted as



It is worth mentioning that the grain potential ϕ_{el} depends on the average charge state of the grain (Z), in addition to its size (a), and mathematically expressed as (Ferland 1996) $\phi_{el} = (Z + 1)e^2/a$.

In a PN DP environment, the grains present in the DP exhibited ionization in the case of lower hydrogen density conditions ($n_H = 10 \text{ cm}^{-3}$), whereas for $n_H > 10 \text{ cm}^{-3}$, it offered promising electron capturing ability (figure 4e–h). Due to a lesser interaction of photons with the DP in a lower hydrogen density regime, the transmitted radiation is more intense. As a consequence, photo-ionization effects of grains could be witnessed in the same regime. The maximum accumulated charge (Z_{max}) due to ionization of grains having working potential (W) may be written as (Fortov *et al.* 2003)

$$Z_{max} = (h\nu_{max} - W)a_p/e^2. \quad (3.6)$$

It is worth mentioning that the photoionized electron temperature does not depend on the radiation flux, but depends on the frequency of it. In accordance with equation (3.6), the positive charge accumulated in PAH grains is more for larger grain size particles, as can be witnessed from figure 4(e). To probe the stability of the grain distribution in space, we studied the variation of kinetic energy of the grains with respect to the charge variation on the grain surface. An increasing trend of grain temperature could be witnessed for higher charge accumulated cases, as depicted in figure S3 (supplementary material). For

the $n_H = 10^4 \text{ cm}^{-3}$ case, grain temperature varies from 80 K to 180 K. Notably, at a fixed charged state, larger grain exhibits a lower velocity.

On the other hand, in higher n_H cases, the radiation flux lowers after interaction with H-clouds and ionized them, which yield significant electron density in those cases. As the electron density is noticeably higher for $n_H > 10 \text{ cm}^{-3}$, which enriches the grain–electron capture probability. The electron densities for different hydrogen density conditions are shown in figure S4 (supplementary material). Upon accumulation of the electrons, the grains became negatively charged, as shown in figure 4(*f–h*). Note that ionization- and electron-capturing ability offer an increasing trend for grain particles, having larger radius (average).

The unusual temperature profile can be attributed due to the electrostatic interactions between the charged PAH grains and the electrons. Due to the charging/discharging process of the PAH grains, it creates a local potential, i.e., suspected for accelerating the electrons, which results in an unusual temperature variation in DP. It is worth mentioning that, on neglecting the grain potential, the T_{net} curve (as per equation (3.3)) varies significantly from the simulated expectations; which ensures the role of grains in the unusual temperature profile.

In the outer region of DP, discharge of grains could be noticed; which eventually withdraws the electrostatic interactions between the electron and grain, causing a noticeable fall in electron temperature.

4. Conclusion

To conclude, the photoionization effects have been studied in DP, located around any arbitrary PN, with core temperature 10^5 K . In the inner face of the DP cloud, owing to the direct interaction of the radiation flux, the ionization factor $\chi(H)$ becomes as high as ~ 1 . For higher n_H cases, this value follows a declining trend with respect to the depth of the DP cloud. Apart from monotonic lowering of temperature for $n_H = 10 \text{ cm}^{-3}$, an interesting unusual trend of the temperature profile could be recorded for $n_H > 10 \text{ cm}^{-3}$. In lower hydrogen density conditions, photoionization of PAH grains is most prominent; whereas the electron capture probability of PAH grains boost up in higher n_H conditions. The electrostatic interactions between the charged PAH grains and the electrons are speculated for the unusual temperature variation in a DP environment.

Supplemental material

Supplementary material is available at <https://doi.org/10.1017/S0022377824001697>.

Acknowledgements

The author is thankful to Ms. Lucky Saikia, Research Scholar, CPP, Sonapur for useful discussions. The author also acknowledges the computational facility provided by the Department of Physics, Morigaon College, Morigaon, Assam, India.

Editor E. Thomas, Jr. thanks the referees for their advice in evaluating this paper.

Declaration of interests

The author reports no conflict of interest.

REFERENCES

- ABID, A.A., ALI, S. & MUHAMMAD, R. 2013 Dust grain surface potential in a non-Maxwellian dusty plasma with negative ions. *J. Plasma Phys.* **79** (6), 1117–1121.

- COX, N.L.J., PILLERI, P., BERNÉ, O., CERNICHARO, J. & JOBLIN, C. 2015 Polycyclic aromatic hydrocarbons and molecular hydrogen in oxygen-rich planetary nebulae: the case of NGC 6720. *Mon. Not. R. Astron. Soc.: Lett.* **456** (1), L89–L93.
- DALGARNO, A. & LAYZER, D. (Eds.). 1987 *Spectroscopy of Astrophysical Plasmas*, vol. 7. Cambridge University Press.
- FERLAND, G.J. 1996 HAZY, a brief introduction to CLOUDY 90. University of Kentucky Internal Report.
- FERLAND, G.J., CHATZIKOS, M., GUZMÁN, F., LYKINS, M.L., VAN HOOF, P.A.M., WILLIAMS, R.J.R., ABEL, N.P., BADNELL, N.R., KEENAN, F.P., PORTER, R.L. & STANCIL, P.C. 2017 The 2017 release of CLOUDY. *Rev. Mex. Astron. Astrofis.* **53** (2), 385–438.
- FERLAND, G.J., KORISTA, K.T., VERNER, D.A., FERGUSON, J.W., KINGDON, J.B. & VERNER, E.M. 1998 CLOUDY 90: numerical simulation of plasmas and their spectra. *Publ. Astron. Soc. Pac.* **110** (749), 761.
- FORTOV, V.E., NEFEDOV, A.P., VAULINA, O.S., PETROV, O.F., DRANZHEVSKI, I.E., LIPAEV, A.M. & SEMENOV, Y.P. 2003 Dynamics of dust grains in an electron–dust plasma induced by solar radiation under microgravity conditions. *New J. Phys.* **5** (1), 102.
- GOREE, J. 1992 Ion trapping by a charged dust grain in a plasma. *Phys. Rev. Lett.* **69** (2), 277.
- GÜÉMEZ, J. & FIOLEHAIS, M. 2018 Relativistic description of the photoelectric effect. *Am. J. Phys.* **86** (11), 825–830.
- GUZMAN-RAMIREZ, L., ZIJLSTRA, A.A., NÍCHUIMÍN, R., GESICKI, K., LAGADEC, E., MILLAR, T.J. & WOODS, P.M. 2011 Carbon chemistry in Galactic bulge planetary nebulae. *Mon. Not. R. Astron. Soc.* **414** (2), 1667–1678.
- LIU, X.W. & DANZIGER, J. 1993 Electron temperature determination from nebular continuum emission in planetary nebulae and the importance of temperature fluctuations. *Mon. Not. R. Astron. Soc.* **263** (1), 256–266.
- MEIXNER, M., ARENS, J.F., JERNIGAN, J.G., BALL, J.R. & SKINNER, C.J. 1993 Mid-IR (8–13 μ M) images of planetary nebulae. In *Symposium-International Astronomical Union*, vol. 155, p. 211. Cambridge University Press.
- MENDIS, D.A. & ROSENBERG, M. 1994 Cosmic dusty plasma. *Annu. Rev. Astron. Astrophys.* **32** (1), 419–463.
- SAINTONGE, A. & CATINELLA, B. 2022 The cold interstellar medium of galaxies in the Local Universe. *Annu. Rev. Astron. Astrophys.* **60**, 319–361.
- SALZ, M., BANERJEE, R., MIGNONE, A., SCHNEIDER, P.C., CZESLA, S. & SCHMITT, J.H.M.M. 2015 TPCI: the PLUTO-CLOUDY Interface-A versatile coupled photoionization hydrodynamics code. *Astron. Astrophys.* **576**, A21.
- STASIŃSKA, G. & SZCZERBA, R. 2001 The temperature structure of dusty planetary nebulae. *Astron. Astrophys.* **379** (3), 1024–1038.
- TIELENS, A.G.G.M. & ALLAMANDOLA, L.J. 1987 Evolution of interstellar dust. In *Physical Processes in Interstellar Clouds*, 1st ed. (eds. G.E. Morfill & M. Scholer), vol. 210, pp. 333–376. Springer.
- UZDENSKY, D.A. & RIGHTLEY, S. 2014 Plasma physics of extreme astrophysical environments. *Rep. Prog. Phys.* **77** (3), 036902.
- WOOD, B.E. & LINSKY, J.L. 1997 A new measurement of the electron density in the local interstellar medium. *Astrophys. J.* **474** (1), L39.